Stability of operation versus temperature of a three-phase clock-driven chaotic circuit*

Zhou Ji-Chao(周继超)[a], Hyunsik Son[a], Namtae Kim[b], and Han Jung Song[a)c)†]

[a)] *Department of Nano Systems Engineering, Inje University, Gimhae* 621-749, *Korea*
[b)] *Department of Electronic Engineering, Inje University, Gimhae* 621-749, *Korea*
[c)] *Center for Nano Manufacturing, Inje University, Gimhae* 621-749, *Korea*

(Received 3 August 2013; revised manuscript received 17 September 2013)

We evaluate the influence of temperature on the behavior of a three-phase clock-driven metal–oxide–semiconductor (MOS) chaotic circuit. The chaotic circuit consists of two nonlinear functions, a level shifter, and three sample and hold blocks. It is necessary to analyze a CMOS-based chaotic circuit with respect to variation in temperature for stability because the circuit is sensitive to the behavior of the circuit design parameters. The temperature dependence of the proposed chaotic circuit is investigated via the simulation program with integrated circuit emphasis (SPICE) using 0.6-μm CMOS process technology with a 5-V power supply and a 20-kHz clock frequency. The simulation results demonstrate the effects of temperature on the chaotic dynamics of the proposed chaotic circuit. The time series, frequency spectra, bifurcation phenomena, and Lyapunov exponent results are provided.

Keywords: chaotic circuit, nonlinear functions, temperature effect, bifurcation, Lyapunov exponent

PACS: 05.45.Gg, 82.40.Bj, 85.40.–e, 05.45.–a **DOI:** 10.1088/1674-1056/22/12/120506

1. Introduction

Since Pecora and Carrol proposed a method to synchronize two identical chaotic systems,[1,2] chaotic circuits and their applications in secure communication have attracted the great attention from many researchers. In addition, secure communication using a chaotic signal (as a carrier) to mask sensitive information has been successfully demonstrated.[3,4] The main advantage of chaotic secure communication system in comparison with conventional cryptosystems is that chaotic secure communication systems can be realized with very simple circuits on part of a chip.[5] As reported by Yang,[6] fourth-generation chaos-based secure communication, which uses impulsive synchronization, has a greater advantage over third-generation chaos-based secure communication, which uses continuous chaotic synchronization.[7–9] Lower bandwidth usage (performance in a limited bandwidth) is needed to transmit the synchronization signal, which is less sensitive to channel noise and provides a much higher degree of security.[6] Furthermore, hardware implementations using integrated circuits based on CMOS technology have become popular instead of using discrete electronic components, because these integrated circuits are much more convenient for compact, effective, and low-cost embedded systems.[10,11]

In chaos-based secure communication using impulsive synchronization, discrete-time chaotic generators act as a critical and essential role and determine the performance of the overall system. This has led to discrete chaotic generators that have attracted much attention in the field of electronics engineering. Intensive studies have been conducted on the implementation of chaotic systems.[12] These circuits are very useful because they represent new types of random generators that can be used for secure communication and neural networks.[13–16]

The most important aspect in the design of a chaotic circuit is the design of the nonlinear functions (NFs) by considering the relationships among the circuit parameters. The variations in these critical parameters can eliminate the output chaotic sequence of the circuit.[17] However, both analog and digital integrated circuits based on silicon are highly sensitive to temperature.[18–23] For chaotic applications, temperature-stable chaotic systems are required; therefore, the temperature dependence on the chaotic dynamics of these circuits needs to be analyzed sufficiently. In previous designs, the effects of temperature were ignored,[5,10,11,16] raising the issue of what will happen if the operating temperature is changed within a large range. Therefore, the temperature dependences of the chaotic dynamics of these circuits must be thoroughly analyzed. In this work, we propose a three-phase clock-driven chaotic oscillator by voltage control based on CMOS technology and then analyze the effects of temperature on the operation of the circuit. The temperature range chosen in this study is from −60 °C to 60 °C, which covers realistic operating conditions.

The remainder of this paper is organized as follows. In Section 2, we propose a simple three-phase chaotic circuit,

*Project supported by the Basic Science Research Program through the National Research Foundation of Korea (NRF) funded by the Ministry of Education (Grant No. 2011-0011698).

†Corresponding author. E-mail: hjsong@inje.ac.kr

© 2013 Chinese Physical Society and IOP Publishing Ltd

analyze the circuit topology, and generate the discrete chaos equations. In Section 3, we perform the analyses of the effects of temperature on the transfer curves of the chaotic circuit using an approximate mathematical model. In Section 4, we present the simulation results of the desired operation at room temperature and then demonstrate undesired effects due to temperature variation. Finally, in Section 5, we discuss our conclusions with several comments regarding the design of the CMOS-based discrete chaotic circuit.

2. Three-phase clock-driven chaotic circuit for the analysis of the effects of temperature

In this study, a three-phase clock-driven chaotic oscillator is proposed for temperature analysis. Figure 1(a) shows the block diagram, and figure 1(b) shows the schematic diagram of the proposed chaotic circuit.

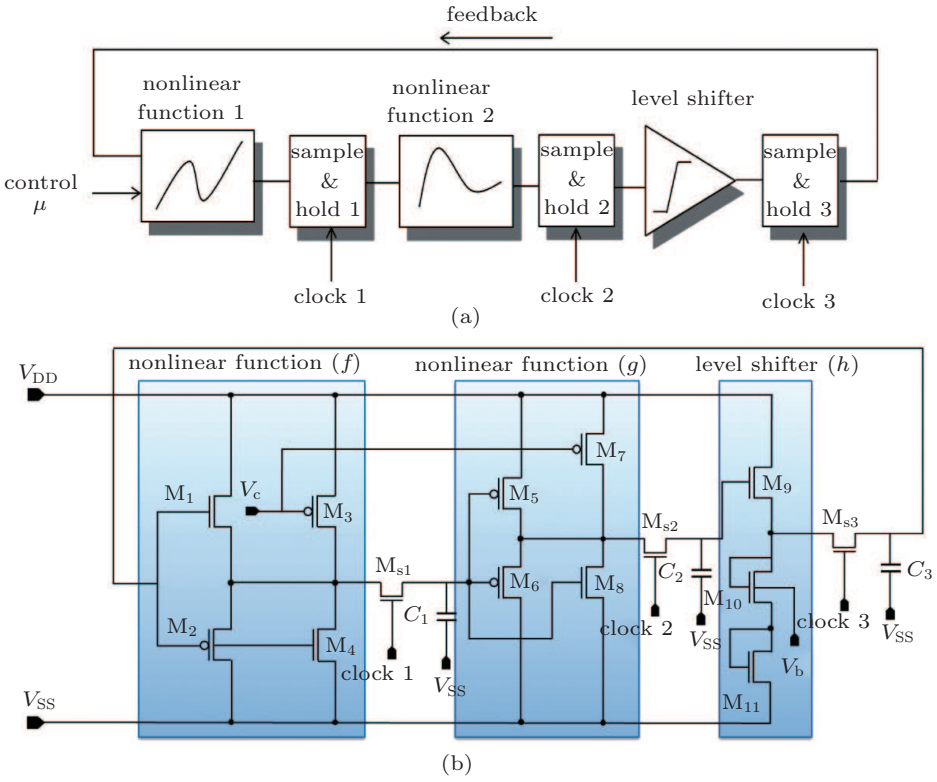


Fig. 1. (color online) (a) Block diagram and (b) three-phase clock-driven chaotic oscillator.

From Fig. 1(a), the entire circuit model is described by

$$x(t+1) = h \cdot g \cdot f(x(t-2), \mu), \tag{1}$$

where x is the internal state variable, μ is the control factor, g and f are the nonlinear functions (NFs) that generate a chaos map, and h is a linear function that represents the buffer. Figure 1(b) shows the implementation of Fig. 1(a), where two NFs are realized using two sub-circuits to generate a chaos map.[24] The chaos map is controlled by the voltage, which determines whether the chaotic circuit generates a chaotic or periodic signal. Further, a level shifter (LS) is used as a buffer to adjust the output voltage for feedback.[10] In addition, three sample and hold blocks, which act as capture and delay elements, are used to generate the discrete time series. These clocks need to ensure that the overlapping between them does not occur.

Figures 2(a) and 2(b) show the transfer curves of the two sub-circuits that generate the chaos map, and figure 2(c) shows the transfer curve of the LS, which is biased at a fixed voltage ($V_b = 0.9$ V).

The operation of the proposed circuit is described as follows (Fig. 1). When clock 1 is active, the output of nonlinear block 1 is sampled and stored in C_1. In the next time steps (i.e., when clock 2 is active), the sampled voltage is captured at the output of nonlinear function block 2 (NFB2) (stored in C_2) and finally at the output of the LS (stored in C_3), which is feedback to the input according to Eq. (1) to generate a sequence of output signals. The computation is iterated once per cycle; thus, a discrete dynamic system is generated by continuous cycles to generate an iterated map from the implementation of Eq. (1).

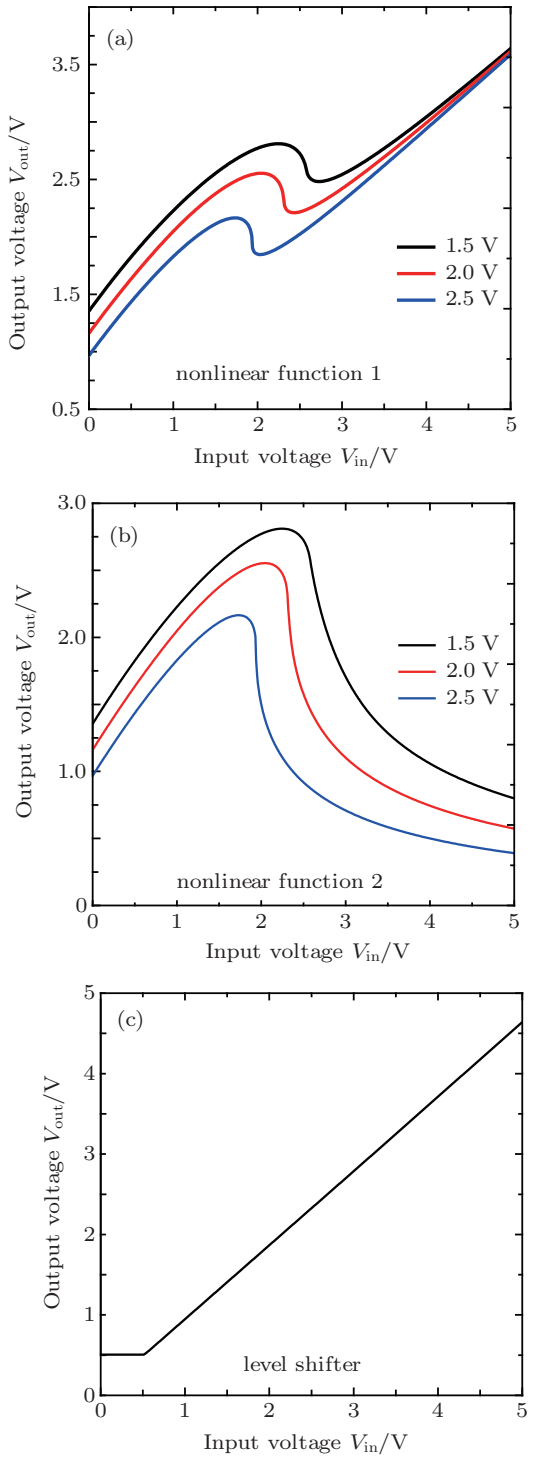


Fig. 2. (color online) Transfer curves at room temperature for (a) NF block 1, (b) NF block 2, and (c) LS block.

3. Effects of temperature on the discrete-time chaotic circuit

3.1. Temperature dependence on the properties of MOSFET

For stable operation of a chaotic circuit, all noise source types must be considered and their effects on the dynamic range must be evaluated. Hence, a comprehensive study on the effects of temperature on the integrated chaotic circuit is not only fundamental but also critical. This is because of the sensitivity of the initial conditions of any chaotic system. First, we introduce the effects of temperature on the properties of metal–oxide–semiconductor field-effect transistor (MOSFET) devices. Then, the undesirable effects of the variation in temperature on the operation of the system is discussed with the aid of the transfer curves.

A metal–oxide–semiconductor (MOS) transistor exhibits a temperature dependence that must be considered in circuit designs. Many studies have been conducted to evaluate the effects of temperature on the characteristics of MOS devices.[21,25–28] In MOS technology, many temperature-dependent parameters are needed, such as mobility, threshold voltage, saturation velocity, series parasitic resistance, leakage current, output resistance, and sub-threshold current.[21,27] The two most important basic parameters of a MOSFET, i.e., the mobility and threshold voltage, have been thoroughly analyzed with regard to the temperature variation. For simplicity, we focus on these factors to highlight the effects on the characteristics of MOSFET devices due to temperature.

The mobility values of the charge carriers (electrons and holes) are determined by several scattering mechanisms: phonon scattering (by optical and acoustical phonons), ionized impurity scattering, surface scattering, remote charge scattering, etc. Phonon scattering is strongly temperature-dependent because the number (density) of phonons increases with temperature increasing (i.e., this density follows the Bose–Einstein distribution). This causes the mobility to be temperature-dependent.

Following Ref. [27], we write the n-channel transistor drain current equations (with neglecting the effects of channel length) as follows:

in the saturation region,

$$I_{\mathrm{d}} = \frac{\mu_{\mathrm{n}} C_{\mathrm{ox}}}{2}\left(\frac{W}{L}\right)(V_{\mathrm{GS}} - V_{\mathrm{T}})^2; \tag{2}$$

in the Ohmic (triode) region,

$$I_{\mathrm{d}} = \frac{\mu_{\mathrm{n}} C_{\mathrm{ox}}}{2}\left(\frac{W}{L}\right)\left[2(V_{\mathrm{GS}} - V_{\mathrm{T}})V_{\mathrm{DS}} - V_{\mathrm{DS}}^2\right]. \tag{3}$$

In this equation, μ_{n} is the carrier mobility, and V_{T} is the threshold voltage, which decreases with the increase of temperature.[29] As reported in Refs. [29] and [30], these quantities are expressed as functions of temperature as follows:

$$V_{\mathrm{T}}(T) = V_{\mathrm{T}}(T_0) + \alpha_{VT}(T - T_0), \tag{4}$$

$$\mu_{\mathrm{n}}(T) = \mu_{\mathrm{n}}(T_0)\left(\frac{T}{T_0}\right)^{\alpha_\mu}, \tag{5}$$

where T_0 is the reference temperature (or absolute temperature at 300 K or 27 °C), $\alpha_{\mathrm{VT}} = \partial V_{\mathrm{T}}/\partial T$, and α_μ is a negative constant. At high drain currents, we consider the current when the gate–source voltage V_{GS} is above the threshold voltage. In both the saturation region and Ohmic region, the drain–source

current I_d is controlled by the carrier mobility and threshold voltage. Keep in mind that the threshold voltage is also a function of temperature and decreases with temperature increasing as shown in Eq. (4); however, the variation in mobility dominates compared with the variation in the threshold voltage with temperature increasing,[29] so that the drive current decreases as temperature increases. This effect is illustrated in Figs. 3(a) and 3(b). At low drain current, the variations in surface inversion potential (affecting the threshold voltage) with temperature will dominate the temperature-induced changes in drain current, meaning that the drain current decreases as the temperature decreases as shown in the inset of Fig. 3(a). In addition, the MOS output resistance usually increases as temperature increases.

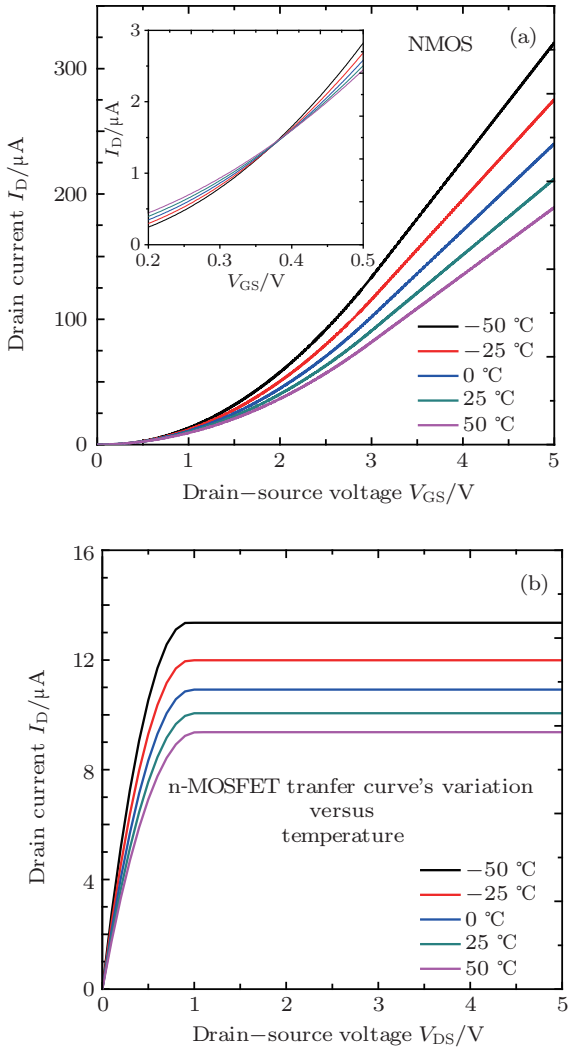


Fig. 3. (color online) Variations in the current–voltage characteristics of an n-type MOSFET with temperature, showing (a) I_d–V_{gs} and (b) I_d–V_{ds}.

The simulation results above confirm the temperature dependence of the MOSFET. Based on this fundamental understanding, we evaluate the variations of the transfer curves of a MOSFET based on a chaotic circuit and then demonstrate their effects on the unstable behavior of a chaotic system.

3.2. Temperature dependence of the characteristics of MOSFET-based chaotic circuit

The simplest way to study the effects of temperature on the operation of the proposed chaotic circuit is to observe their influences on the transfer curves of the entire chaotic circuit. However, this is very complex work that cannot be

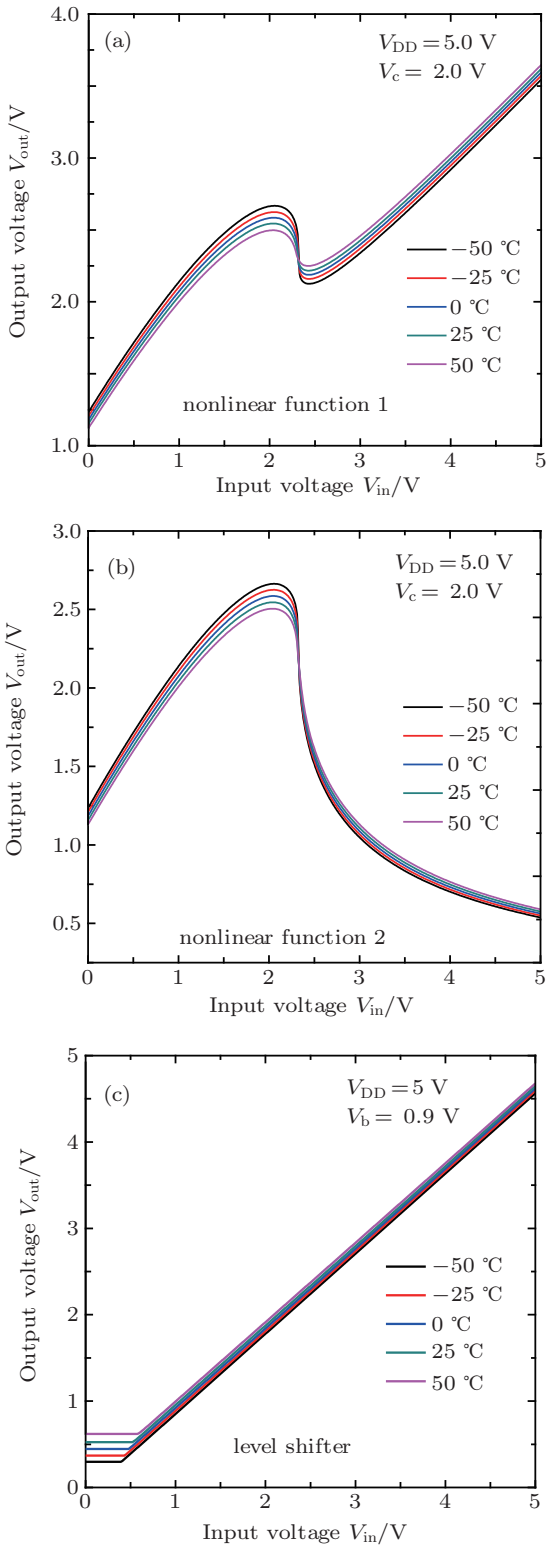


Fig. 4. (color online) Variations of transfer curves with temperature for (a) NF block 1, (b) NF block 2, and (c) LS block.

accomplished by hand-calculations. Thus, we limit our study to evaluating the effects of temperature and their importance on MOSFET-based chaotic circuit design. This study is supported by the SPICE program. Figure 4 shows the variations in the transfer curves with temperature.

To evaluate the effects of temperature on the behavior of the circuit, we assume that the circuit operates in a temperature range from –50 °C to 50 °C, which is the realistic operating condition. The function exhibits a temperature-sensitive family of curves as shown in Fig. 4(a). The transfer curves for different temperatures exhibit N-type shapes and negative differential resistance in an input range from 2.25 V to 2.45 V. The second function exhibits temperature-sensitive bell-shaped transfer characteristics and negative differential resistance in an input range from 2.25 V to 5.0 V [Fig. 4(b)]. Finally, figure 4(c) shows that the LS exhibits temperature-sensitive linear transfer curves with a dropout voltage on the order of hundreds of millivolts. Here, the temperature variation causes a slight modification to each of the transfer curves in the sub-blocks. However, these slight variations of these curves significantly affect the chaotic dynamics of the circuit.

From the simulated data in Fig. 4, the transfer curves are expressed as follows:

$$f(x)=\begin{cases} 0.72018x+1.26734+\alpha_1, & 0\le x<2,\\ -0.29066x+3.15274+\alpha_2, & 2\le x<2.25,\\ -1.36639x+5.49724+\alpha_3, & 2.25\le x<2.45,\\ 0.57361x+0.71107+\alpha_4, & 2.45\le x<5, \end{cases} \tag{6}$$

$$g(x)=\begin{cases} 0.72018x+1.26734+\beta_1, & 0\le x<2,\\ -0.29066x+3.15274+\beta_2, & 2\le x<2.25,\\ -2.30261x+7.44888+\beta_3, & 2.25\le x<2.75,\\ -0.28311x+1.91592+\beta_4, & 2.75\le x<5, \end{cases} \tag{7}$$

$$h(x)=\begin{cases} 0.50587+\gamma_1, & 0\le x<0.5,\\ 0.92236x+0.02315+\gamma_2, & 0.5\le x<5, \end{cases} \tag{8}$$

where α_i $(i=1:4)$, β_j $(j=1:4)$, and γ_k $(k=1:2)$ are the empirically fitted temperature-coefficient factors of the functions that show the changes in behaviors of the transfer curves according to temperature variation. We note that all the functions behave approximated as piecewise linear functions. These empirical equations can be thought of as a simple way to determine the effects of temperature, rather than to solve the more complex equations of small-signal models.

4. Simulation results

The circuit is analyzed via SPICE simulation with a 5-V power supply and a 20-kHz clock frequency. We first verify the operation of the proposed chaotic circuit at room temperature (25 °C), and then evaluate the effects of temperature.

To verify the chaotic properties of the discrete-time chaotic circuit, a set of numerical experiments including time series, frequency spectrum, bifurcation, and Lyapunov exponent analysis are conducted.

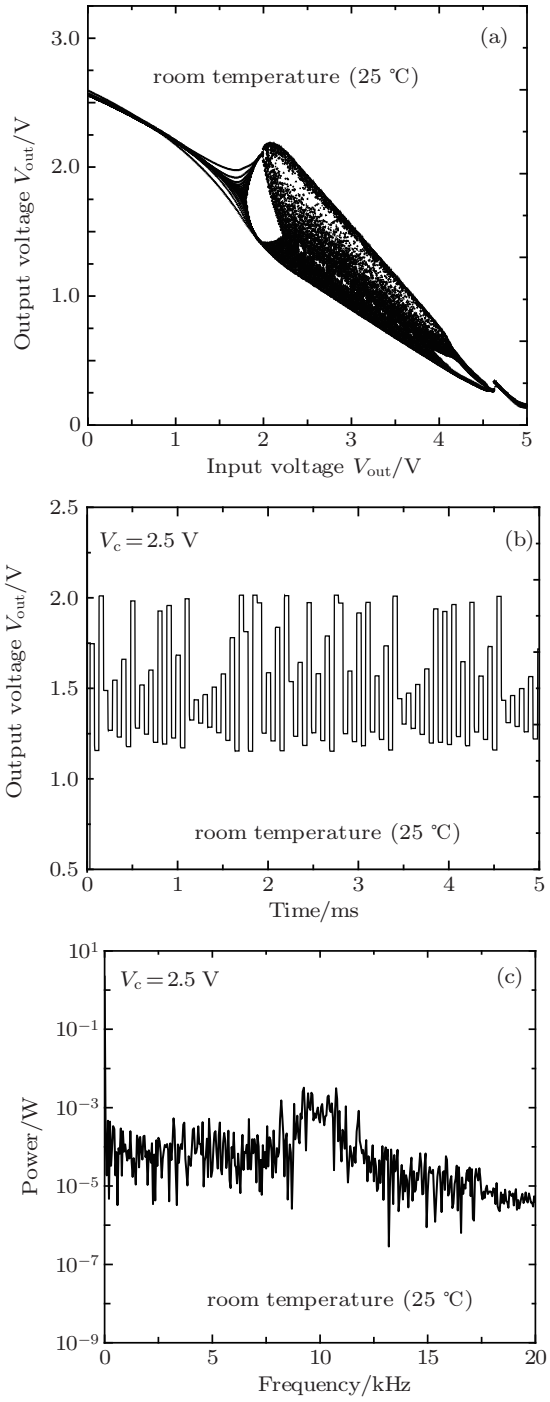


Fig. 5. (a) Bifurcation diagram at room temperature and (b) the chaotic time series at the output, and (c) the chaotic frequency at the output.

SPICE simulations are carried out using the proposed circuit in Fig. 1 to verify the operation of the proposed circuit before analyzing the effects of temperature. In the SPICE simulations, the circuit operates at the control voltage $V_c = 2.5$ V and the temperature 25 °C. In addition, the bias voltage V_b is set to be 0.9 V, which allows the LS to feedback a suitable voltage to generate a chaotic signal. Figure 5(a) shows the chaotic output for a wide range of V_c from 2.3 V to 4 V, whereas the other regions show periodic and equilibrium signals. Figure 5(b) shows a time series of a chaotic signal. Figure 5(c) shows the frequency spectrum for a frequency range

of 0 kHz–20 kHz, which clearly shows one of the chaotic characteristics.

Next, the operation of the proposed circuit is confirmed via the bifurcation diagram, one of the most effective methods of measuring the behavior of a chaotic circuit. Some bifurcation diagrams are presented in this paper to provide an overview of the parameter values in which chaotic attractors can exist. The bifurcation diagrams of $V_{\rm out}$ versus the temperature are shown in Fig. 6, where we can easily see the effects on the operation of the chaotic circuit when temperature varies. The domain of existence for chaos at different temperatures is presented. The variation in temperature, however, can eliminate the chaotic operation of the system; thus, the output behaves in a simple, a periodic, a quasi-periodic, or even an equilibrium state. Here, we perform a simple comparison between Fig. 5(a) and the bifurcation diagrams in Figs. 6(b) and 6(c) in which the temperatures are -25 °C and 0 °C (these conditions can be realized according to environmental conditions or fluctuations at the operating temperature). For $V_{\rm c} = 3$ V, the circuit exhibits a chaotic signal at room temperature, whereas it exhibits a periodic signal at -25 °C [Fig. 6(b)] or an equilibrium signal at -50 °C [Fig. 6(a)].

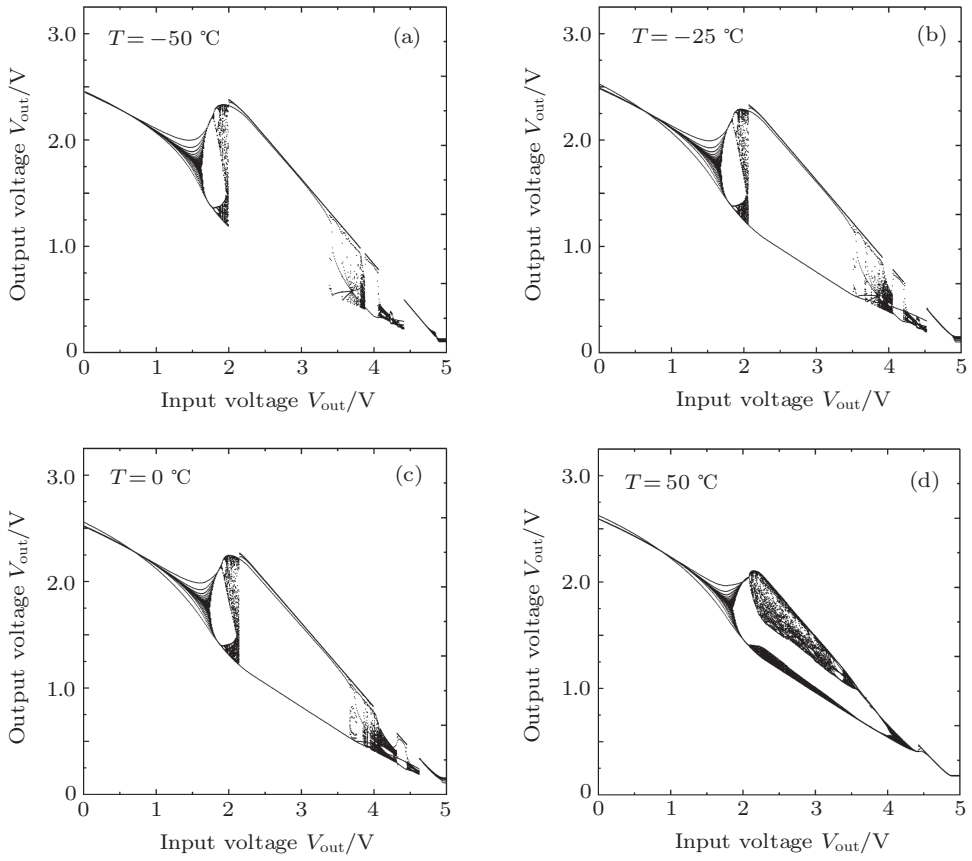


Fig. 6. Bifurcation diagrams of $V_{\rm out}$ versus $V_{\rm c}$ at different temperatures: (a) -50 °C, (b) -25 °C, (c) 0 °C, and (d) 50 °C.

We now analyze the effect of temperature on the operation of the chaotic circuit. To maintain simplicity in the analysis, we consider the temperature as a new control factor; thus, equation (1) can be represented as follows:

$$x(t+1) = h \cdot g \cdot f(x(t-2), \mu, \phi), \tag{9}$$

where ϕ is a control variable that represents the temperature coefficient [other variables have the same definitions as those in Eq. (1)]. We assume that the chaotic circuit is designed to generate a four-period signal at the output at room temperature [Fig. 5(a)]. Then, we measure the output variation when the temperature varies from -60 °C to 60 °C. Figure 7(a) shows that the output of the chaotic signal changes considerably and exhibits almost all the behaviors (in equilibrium, periodic, quasi-periodic, and chaotic signals) that a chaotic system should have. Figure 8 shows the output variations at two different temperatures. Figures 8(a) and 8(b) show the time series and frequency spectrum of the chaotic state at -40 °C. Figure 8(b), which corresponds to Fig. 8(a), shows the frequency spectrum for a frequency range of 0 kHz–20 kHz. Furthermore, figures 8(c) and 8(d) show the time series and frequency spectrum of the six-period state at 0 °C. Figure 8(d), which corresponds to Fig. 8(c), shows five peaks indicating six periods. The temperature variations cause performance to mismatch between the designed function and the obtained results, leading to functional failure in the operation of the proposed chaotic circuit.

To perform further analyses, Lyapunov exponents for dif-

ferent parameters are needed to confirm systems which own the chaotic behaviors. Lyapunov exponents provide empirical evidence of chaotic behavior. In general, the values of Lyapunov exponents are usually computed using two different methods. The first method is used for continuous systems that Lyapunov exponent is defined as follows:[10]

$$\lambda = \int \log \left| f'(x) \right| \rho(x)\, \mathrm{d}x. \tag{10}$$

In this definition it is assumed that the differential function $f(x)$ and the distribution function $\rho(x)$ must be known. However, we need to estimate the value of the Lyapunov exponent numerically based on the samples of the output voltages obtained in the simulation for each particular value of temperature parameter. The Lyapunov exponent is then calculated according to the following equation:[31]

$$\lambda = \frac{1}{N} \sum_{n=0}^{N-1} \log_2 \left| \frac{\Delta x_i (t_\mathrm{n} + 1)}{\Delta x_i (t_\mathrm{n})} \right|. \tag{11}$$

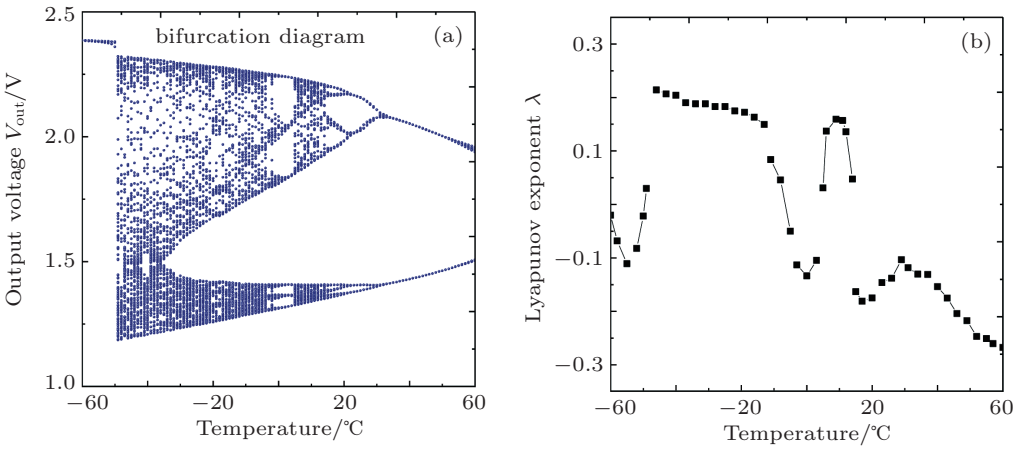


Fig. 7. (color online) Bifurcation diagrams of V_{out} and Lyapunov exponent diagram versus temperature (V_c is fixed at 2 V).

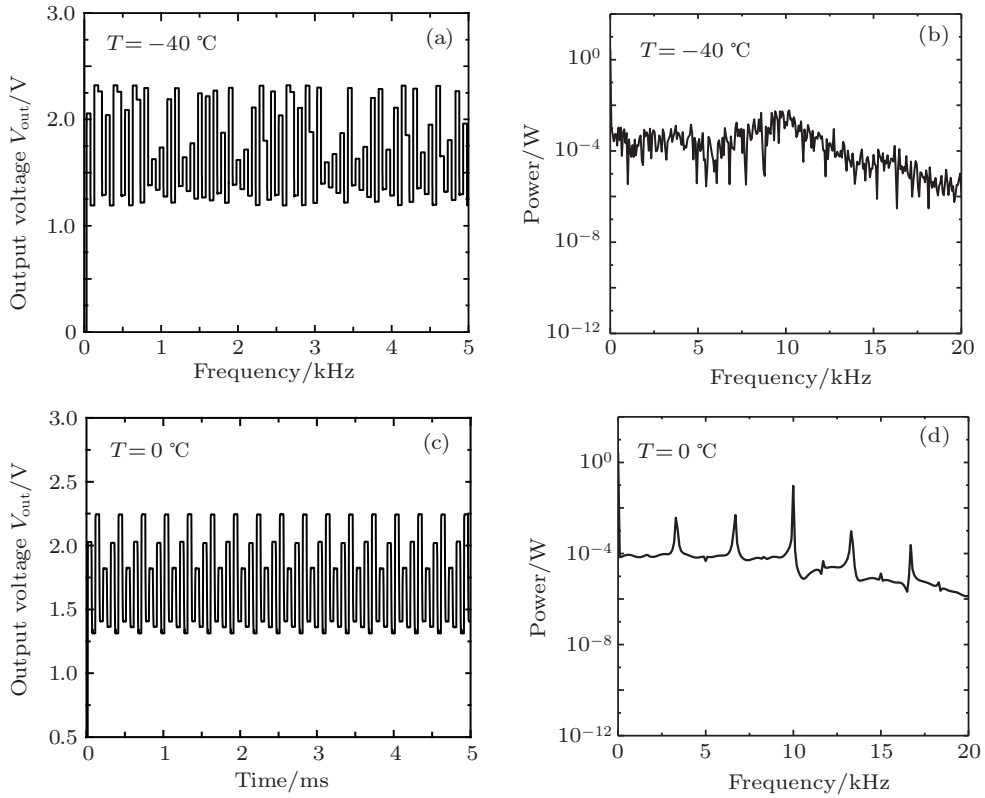


Fig. 8. Output voltages varying with time at temperatures of −40 °C (a) and 0 °C (c), and output powers varying with frequency at temperatures of −40 °C (b) and 0 °C (d) (V_c is fixed at 2 V).

It should be noted that the calculated values of Lyapunov exponents in Eq. (11) for various values of temperature gain high precision in the case where the number of data of internal state x_i of time series is large enough. This affects the accuracy of the calculated Lyapunov exponent. A plot of Lyapunov exponent values, calculated for various values of temperature is shown in Fig. 7(a) with 12000 points of the internal states from $x[0]$ to $x[12000]$. The behavior of circuit now is confirmed by a positive Lyapunov exponent, which indicates that the series is chaotic while the others with negative values represent non-chaotic output signal (periodic or equilibrium signal). For instance, for $T = 40$ °C the Lyapunov exponent is calculated to be equal to -0.1537. This is matched with the time series at the output as shown in Fig. 7(b). All these gained results confirm that the temperature variations cause a mismatch performance between the designed function and the obtained result on output, leading to functional failure in the operation of the proposed chaotic circuit.

As mentioned at the beginning of this paper, the proposed chaotic circuit is designed using the MOS technology which heavily depends on the operating temperature. This is an important and critical problem as it is not easy to eliminate the temperature dependence of a conventional MOS-based chaotic circuit. However, a feasible solution is to design the circuits which need to be stable against the temperature by means of the merits of new materials in combination with the hardware design technology,[32] for high quality chaotic generators in the future.

5. Conclusion

The effects of temperature on the behavior of a discrete-time-based chaotic circuit are investigated by using SPICE simulations with 0.6-μm CMOS technology. The simulation results demonstrate the effects of temperature on the operation of the proposed chaotic circuit. Therefore, in the design of the integrated chaotic oscillators, the effects of temperature must be taken into consideration.

References

[1] Pecora L M and Carroll T L 1990 *Phys. Rev. Lett.* **64** 821

[2] Pecora L M and Carroll T L 1991 *IEEE Trans. Circ. Sys.* **38** 453

[3] Dedieu H, Kennedy M P and Hasler M 1993 *IEEE Trans. Circ. Syst. II* **40** 634

[4] Corron N J and Hahs D W 1997 *IEEE Trans. Circ. Syst. I* **44** 373

[5] Rosselló J L, Canals V, Paul I D and Bota S A 2008 *IEICE Electronics Express* **5** 1042

[6] Yang T 2004 *Int. J. Comp. Cognit.* **2** 81

[7] Puebla H and Alvarez-Ramirez J 2001 *Phys. Lett. A* **283** 96

[8] García-López J H, Jaimes-Reategui R, Chiu-Zarate R, Lopez-Mancilla D, RamirezJimenez R and Pisarchik A N 2008 *The Open Electrical and Electronic Engineering Journal* **2** 41

[9] Liu H J, Ren B and Feng J C 2012 *Chin. Phys. B* **21** 040501

[10] Juncu V D, Rafiei-naeini M and Dudek P 2006 *Analog Int. Circ. Syst.* **46** 275

[11] Dudek P and Juncu V D 2003 *Electron. Lett.* **39** 1431

[12] Gopal S and Lai C Y 2009 *Circ. Syst. Signal Process.* **28** 535

[13] Feki M, Robert B, Gelle G and Colas M 2003 *Chaos, Solitons and Fractals* **18** 881

[14] Kharel R, Busawon K and Ghassemlooy Z 2010 *American Control Conference*, June 30–July 2, 2010, Baltimore, MD, p. 1791

[15] Stavrinides S G, Anagnostopoulos A N, Miliou A N, Valaristos A, Magafas L, Kosmatopoulos K and Papaioannou S 2009 *J. Eng. Sci. Rev.* **2** 82

[16] Zhang Y and Wang X Y 2012 *Chin. Phys. B* **21** 020507

[17] Gregori S and Cabrini A 2005 *48th Midwest Symposium on Circuits and Systems*, August 7–10, 2005, Covington, KY, p. 1498

[18] Govindarajulu S and Prasad T J 2010 *Int. J. Eng. Sci. Tech.* **2** 2248

[19] Zhou J C and Song H J 2013 *Chin. Phys. Lett.* **30** 020201

[20] Vadasz L and Grove A S 1966 *IEEE Trans. Electron. Dev.* **13** 863

[21] Hasanuzzaman M, Islam S K and Tolbert L M 2004 *Solid-State Electron.* **48** 125

[22] Ku J C and Ismail Y 2007 *Circuits and Systems*, 2007, ISCAS 2007, *IEEE International Symposium on* May 27–30, 2007, New Orleans, LA, p. 3736

[23] Kanda K, Nose K, Kawaguchi H and Sakurai T 2001 *IEEE J. Solid-State Circ.* **36** 1559

[24] Vadasz L and Grove A S 1966 *IEEE Trans. Electron. Dev.* **13** 863

[25] Osman A A and Osman M A 1998 *Fourth International High Temperature Electronics Conference,* June 14–18, 1998, Albuquerque, NM, p. 301

[26] Chen Y H, Imai K, Jeng M C, Liu Z H, Chen K and Hu C M 1997 *Semicond. Sci. Tech.* **12** 1349

[27] Jacob Baker R 2010 *CMOS Circuit Design, Layout, and Simulation*, 3rd edn. (New York: Wiley-IEEE Press) p. 143

[28] Cheung T, Butson M J and Yu P K N 2004 *Phys. Med. Biol.* **49** 191

[29] Tsividis Y P 1987 *Operation and Modeling of the MOS Transistor*, 2nd edn. (New York: McGraw-Hill) p. 189

[30] Sakuna N, Muanghlua R, Niemcharoen S and Ruangphanit A 2013 *Kmitl. Sci. Tech. J.* **13** 9

[31] Horio Y, Aihara K and Yamamoto O 2003 *IEEE Trans. Neural Netw.* **14** 1393

[32] Filanovsky I M and Allam A 2001 *IEEE Trans. Circ. Syst. I: Fundam. Theory Appl.* **48** 876